Pyrene aromatic arrays on RNA duplexes as helical templates

Mitsunobu Nakamura,* Yukinori Shimomura, Yukinori Ohtoshi, Kazuhiro Sasa, Haruhisa Hayashi, Hidehiko Nakano and Kazushige Yamana*

Received 19th April 2007, Accepted 8th May 2007
First published as an Advance Article on the web 18th May 2007
DOI: 10.1039/b705933g

RNA oligomers having multiple (2 to 4) pyrenylmethyl substituents at the 2′-*O*-sugar residues were synthesized. UV-melting studies showed that the pyrene-modified RNAs could form duplexes with complementary RNA sequences without loss of thermal stability. Absorption, fluorescence, and circular dichroism (CD) spectra revealed that the incorporated pyrenes projected toward the outside of A-form RNA duplexes and assembled in helical aromatic arrays along the minor grooves of the RNA duplexes. Results of computer simulations agreed with the assembled structures of the pyrenes. The helical pyrene arrays exhibited remarkably strong excimer fluorescence, which was dependent on the sequence contexts of RNA duplexes.

Introduction

DNA and RNA can be used to arrange chromophores in defined spaces and distances. Their self-assembling properties, into duplexes, triplexes, and quadruplexes, may be useful in forming specifically arranged structures.[1–9] Such nanoscale space arrangements are anticipated to be applicable in materials science research and in biotechnology.

Pyrene has attracted particular interest among various aromatic chromophores because of the ease of synthetic conversion and its high quantum efficiency in both monomer and excimer fluorescence.[10–12] Attempts to incorporate multiple pyrenes into DNA and RNA chains have been made using organic or enzymatic synthesis methods.[13–19] π-Stacked structures between pyrenes can be formed in double-stranded or even in single-stranded DNA, which results in characteristic excimer fluorescence due to the interaction between pyrenes in electronically excited states and ground states. Such fluorescence may be utilized in homogeneous biological assays.

We have previously reported that multiple-pyrene-modified oligo(rU_{20})–oligo(rA_{20}) duplexes at consecutive 2′-positions exhibit unusually strong excimer fluorescence.[20] The modified duplexes exhibit exciton-coupled CD signals in the region of the pyrene absorption band (300 to 380 nm), whereas the single-stranded pyrene-modified oligo(rU_{20}) RNAs exhibit only negative induced CD signals. On the basis of the CD and other spectral data, we tentatively determined the pyrene structure to be a helical arrangement of π-aromatics along the RNA double helix. However, the detailed structural features of multiple-pyrene-modified RNA duplexes and the effects of RNA sequences on pyrene association have not yet been determined. This determination is necessary to gain insight into pyrene-modified RNAs for the development of new materials and biotechnological applications.

We describe the structures of the multiple-pyrene-modified RNA duplexes that were characterized by spectroscopic analyses, molecular dynamics (MD) calculations, and CD simulations, and we discuss the pyrene associations along the RNA duplexes.

Department of Materials Science and Chemistry, Graduate School of Engineering, University of Hyogo, 2167 Shosha, Himeji, Hyogo, 671–2201, Japan. E-mail: mitunobu@eng.u-hyogo.ac.jp, yamana@eng.u-hyogo.ac.jp; Fax: (+81) 79-267-4928; Tel: (+81) 79-267-4928

Results

RNA synthesis

The pyrene-modified RNAs and their complements that were used are shown in Chart 1. Introduction of pyrene moieties ($\mathbf{U}_{py}$, $\mathbf{A}_{py}$, and $\mathbf{C}_{py}$ residues) into RNA sequences was carried out by a conventional phosphoramidite method using protected phosphoramidite derivatives of 2′-*O*-(1-pyrenylmethyl)ribonucleosides. $\mathbf{U}_{py}$ was synthesized as previously described.[21] $\mathbf{A}_{py}$ and $\mathbf{C}_{py}$ were prepared from unprotected ribonucleosides and pyrenylmethyl chloride using a base promoted reaction, as shown in Scheme 1. The protected pyrene-modified ribonucleosides were converted by a standard method into their phosphoramidite derivatives. The pyrene-modified RNAs **Pn**s (n = 1–4) have a $\mathbf{U}_{py}$ domain in the middle of the strand. The RNAs **Qn**s (n = 1–4) have a mixed sequence of five bases at each end of rU_{10} containing the $\mathbf{U}_{py}$ domain displaced 1 to 4 bases from the edge of the rU_{10}. The RNAs **Rn**s (n = 1–3) have $\mathbf{U}_{py}$, $\mathbf{A}_{py}$, and $\mathbf{C}_{py}$ units in the middle of the strand.

Thermal dissociation

Helical stability of pyrene-modified RNA duplexes was evaluated by UV-melting studies in a buffer of pH 7 containing 0.1 M NaCl, 0.01 M $NaHPO_4$, and 1 mM EDTA. The melting profiles for all the pyrene-modified RNA duplexes exhibited single-phase transitions similar to those of unmodified RNA duplexes. The melting temperatures (T_m) of the pyrene-modified RNA duplexes are summarized in Table 1. The T_m values of **Pn-X** differ by 1.5–2.5 °C from those of corresponding unmodified RNA duplex **P0-X**. **Qn-Y**s (n = 1–4) melt at temperatures 2.0–3.9 °C higher than **Q0-Y** and **Rn-Z**s (n = 1–3) and melt at temperatures 3.9–7.8 °C lower than **R0-Z**. Pyrene-modified RNA duplexes are therefore stable under conditions for structural observation at

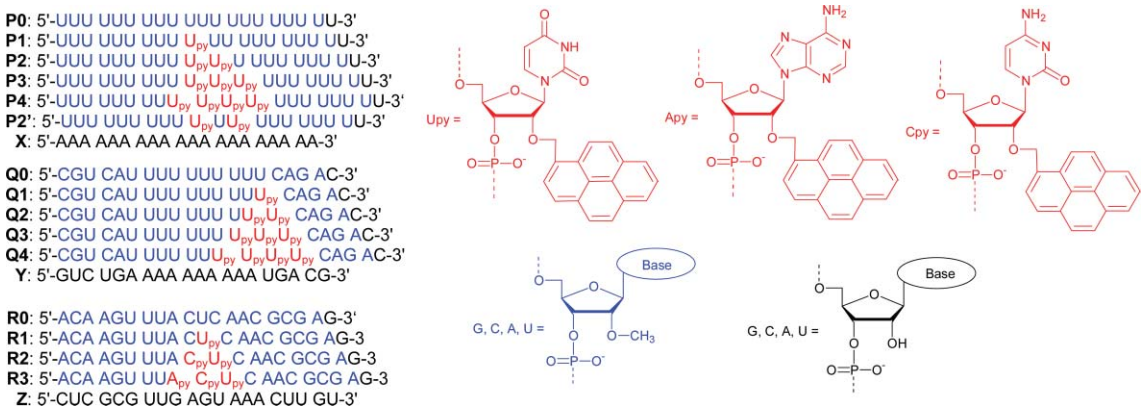

Chart 1 Sequences of pyrene-modified RNAs.

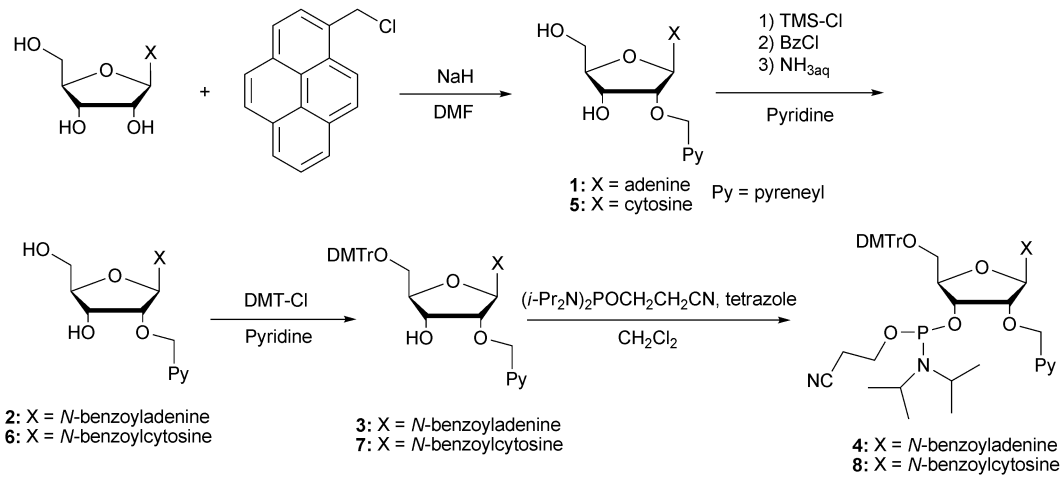

Scheme 1

Table 1 T_m values for pyrene-modified RNA duplexes[a]

Pn-X	T_m/°C	Qn-Y	T_m/°C	Rn-Z	T_m/°C
P0-X	45.0	**Q0-Y**	50.0	**R0-Z**	73.7
P1-X	46.5	**Q1-Y**	53.9	**R1-Z**	69.8
P2-X	47.5	**Q2-Y**	53.9	**R2-Z**	68.9
P3-X	46.6	**Q3-Y**	52.9	**R3-Z**	65.9
P4-X	42.7	**Q4-Y**	52.0		

[a] Measurements were carried out at 260 nm for a 1 : 1 mixture of oligonucleotides with increase in temperature from 20 to 80 °C at a rate of 0.5 °C min^{-1}. Buffer contained 0.01 M sodium phosphate, 0.1 M NaCl, and 1 mM EDTA·2Na adjusted to pH 7.0. The concentration of RNA was 5×10^{-5} M.

Table 2 Absorption maximums (λ_{max}) of pyrene-modified RNAs[a]

RNA	λ_{max}/nm	RNA	λ_{max}/nm	RNA	λ_{max}/nm
P1	348	**Q1**	349	**R1**	349
P1-X	353	**Q1-Y**	352	**R1-Z**	352
P2	348	**Q2**	349	**R2**	348
P2-X	347	**Q2-Y**	350	**R2-Z**	345
P3	349	**Q3**	350	**R3**	349
P3-X	349	**Q3-Y**	350	**R3-Z**	345
P4	349	**Q4**	349		
P4-X	350	**Q4-Y**	349		
P2′	348				
P2′-X	352				

[a] Absorption spectra were measured at room temperature in a buffer containing 0.01 M sodium phosphate, 0.1 M NaCl, and 1 mM EDTA·2Na adjusted to pH 7.0. The concentration of RNA was 5×10^{-5} M.

room temperature. The introduction of multiple pyrenes barely affected the thermal stability of the RNA duplexes.

Absorption spectra

In the absorption spectra of pyrene-modified RNAs, a short-wavelength (about 260 nm) absorption band attributed to the overlapping of nucleobases and pyrenes, and a long-wavelength (300–370 nm) absorption band attributed to the 0–0 absorption for the ^1L_a transition of pyrene, were observed.[22,23] Table 2 summarizes the absorption maximums of the pyrene ^1L_a transition. The single-stranded pyrene-modified RNAs (**Pn**s) exhibited an absorption maximum at a wavelength of 348 to 349 nm. Upon hybridization with complementary RNA, the absorption maximum of **P1** shifted by about 5 nm to a lower energy. In contrast, the pyrene absorption maximum of **Pn**s (n = 2–4) barely shifted upon hybridization.

Similarly, the absorption maximum of single-stranded **Q1** appeared at 349 nm and shifted by about 3 nm to a lower energy upon hybridization with **Y**. The absorption of single-stranded **Qn**s (n = 2–4) and double-stranded **Qn-Y**s (n = 2–4) appeared near 349 nm. In the cases of **Rn**s, the absorption maximum of **R1** shifted to longer wavelengths, but the absorption maximum of **R2** and **R3** shifted to shorter wavelengths upon hybridization with **Z**.

When two pyrenes were separated by one nucleotide in **P′2**, the pyrene absorption band appeared at 348 nm and shifted to 352 nm upon hybridization.

Fluorescence spectra

In the fluorescence spectra of **Pn-X**s reported previously,[20] the monomer intensity of **P1-X** was about 20 times higher than that of **P1**, and the excimer intensities of **Pn-X**s (n = 2–4) were about 1 to 10 times higher than that for single-stranded **Pn**s (n = 2–4).

The fluorescence behavior of **Qn**s and **Rn**s was similar to that of **Pn**s. The mono-pyrene-modified **Q1** exhibited only monomer fluorescence in both single-stranded and double-stranded forms, and the monomer fluorescence intensity in double-stranded **Q1-Y** was about 10 times higher than that in single-stranded **Q1**. The multiple-pyrene-modified **Qn**s (n = 2–4) exhibited weak monomer and excimer fluorescence. The double-stranded **Qn-Y**s (n = 2–4) also exhibited monomer and excimer fluorescence similar to corresponding **Qn**s (n = 2–4) in spectral features, but their fluorescence intensities were about 2 times higher than that of **Qn**s (Fig. 1). Similarly, the fluorescence intensities of **Rn-Z**s were about 1 to 10 times higher than that of **Rn** (Fig. 2).

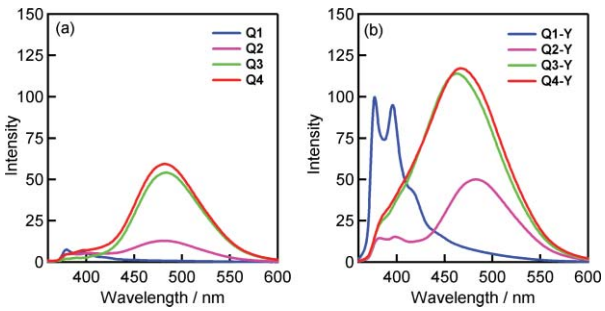

Fig. 1 (a) Fluorescence spectra of **Qn**s (n = 1–4). (b) Fluorescence spectra of **Qn-Y**s (n = 1–4). The measurements were carried out at a strand concentration of 2.5×10^{-6} M at room temperature in a buffer containing 0.01 M sodium phosphate and 0.1 M NaCl, adjusted to pH 7.0. The excitation wavelength was 350 nm.

The fluorescence behavior of **P′2** was different from that of other multiple-pyrene-modified RNAs. Monomer and excimer fluorescence were observed in single-stranded **P′2**. The monomer fluorescence intensity was more than 10 times greater, however, the excimer fluorescence disappeared upon hybridization with **Z** (Fig. 3).

Circular dichroism spectra

CD spectroscopic analyses of the pyrene-modified RNAs were performed to investigate structural preferences. The CD spectra of **Pn**s (n = 1–4) exhibited positive CD signals at wavelengths shorter than 300 nm and negative induced CD signals in the region of 300 to 360 nm.[20] On the other hand, the CD spectra of double-stranded

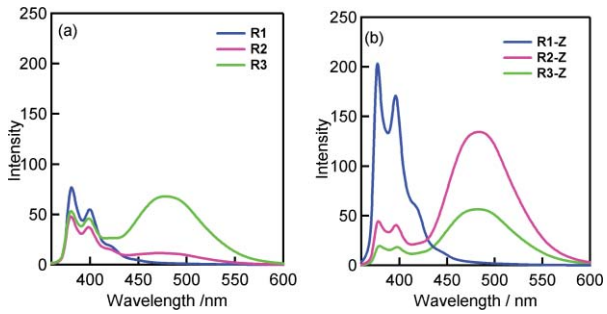

Fig. 2 (a) Fluorescence spectra of **Rn**s (n = 1–3). (b) Fluorescence spectra of **Rn-Z**s (n = 1–3). The measurements were carried out at a strand concentration of 2.5×10^{-6} M at room temperature in a buffer containing 0.01 M sodium phosphate, 0.1 M NaCl, and 1 mM EDTA·2Na adjusted to pH 7.0. The excitation wavelength was 350 nm.

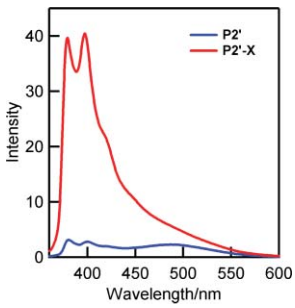

Fig. 3 Fluorescence spectra of **P2′** and **P2′-X** (strand concentration of 2.5×10^{-6} M) at room temperature in a buffer containing 0.01 M sodium phosphate, 0.1 M NaCl, and 1 mM EDTA·2Na adjusted to pH 7.0. The excitation wavelength was 350 nm.

Pn-Xs (n = 2–4) exhibited CD signals due to right-handed A-form RNA below 300 nm and positive Cotton effects attributed to exciton coupling between pyrenes in the region of 300 to 360 nm.[24] The profiles of the exciton coupled CD signals for **Pn-X** (n = 2–4) were very similar to each other, and the intensities of the signals increased with the number of incorporated pyrenes.

Fig. 4 shows the CD spectra of **Qn-Y**s (n = 1–4) and **Rn-Z**s (n = 1–3) at room temperature. The CD profiles below 300 nm for all the pyrene-modified duplexes were similar to that of a typical right-handed A-form RNA. The exciton-coupled CD signals in

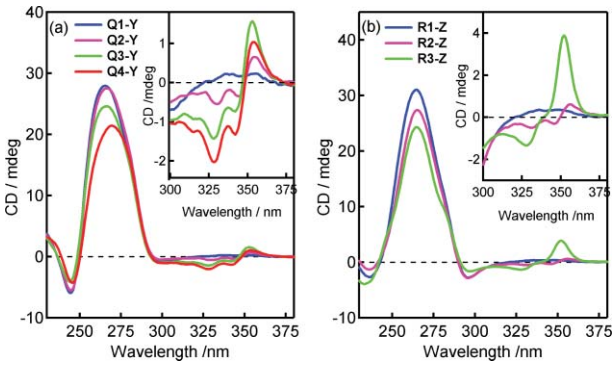

Fig. 4 (a) CD spectra of **Qn-Y**s (n = 1–4). (b) CD spectra of **Rn-Z**s (n = 1–3). The measurements were carried out at a strand concentration of 2.5×10^{-6} M at room temperature in a buffer containing 0.01 M sodium phosphate, 0.1 M NaCl, and 1 mM EDTA·2Na adjusted to pH 7.0.

the region of 300 to 360 nm were observed for multiple-pyrene-modified **Qn-Y**s ($n = 2$–4) and **Rn-Z**s ($n = 2$–3).

Discussion

For the mono-pyrene-modified RNAs, the pyrene absorption band shifted to longer wavelengths and the pyrene-monomer fluorescence was enhanced upon hybridization. These results indicate that the pyrene was free of interactions with nucleobases and that the environment changed from hydrophobic to hydrophilic by hybridization. Hence, the pyrene was located outside of the double helix without intercalation.[25] For the multiple-pyrene-modified RNA, the excimer fluorescence was enhanced upon hybridization, and the pyrene absorption band in double-stranded form appeared at shorter wavelengths than that of the corresponding mono-pyrene-modified RNA duplex. These spectroscopic behaviors suggest that the pyrenes in the multiple-pyrene-modified RNA duplex were located outside the double helix and were associated with each other as an H-aggregate, which induces hypsochromic shift of the absorption band.[2] On the other hand, the two pyrenes were located outside the duplex, without association in **P2′-X**, because the pyrene absorption band appeared at longer wavelengths than that of single-stranded **P2′** and the excimer fluorescence observed in **P2′** disappeared upon hybridization.

We ran simulations of the MD of multiple-pyrene-modified RNA duplexes to clarify the structural features of the assembled pyrenes. The model structure for pyrene-modified RNA duplexes was constructed based on an A-form RNA duplex using the sequence of **P4-X**. The modified duplex was then optimized, thermalized (300 K), and equilibrated using an AMBER module.[26] Fig. 5 shows the energy-minimized structure of **P4-X**. It can be seen that the four pyrenes of **P4-X** projected into the minor groove and were associated approximately parallel with each other. The average center-to-center distance between the two neighboring pyrenes was 6.5 Å. The MD simulations were then performed with an appropriate force field in which the equilibrated structures were subjected to 1 ns (1 000 000 steps) in the simulations at constant temperature (300 K) and pressure (1 atm) with standard relaxation times of 1 fs. We found that whereas the multiple-pyrene-modified RNA duplex rigidly retained its original A-form structure, the center-to-center distances between two adjacent pyrenes changed considerably.

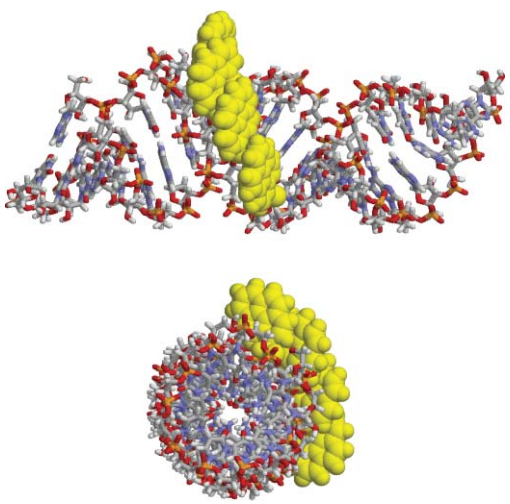

Fig. 5 MD minimized structure of **P4-X**.

The experimentally observed CD assigned to the exciton coupling among the pyrenes in **P4-X** was theoretically evaluated using the exciton-chirality method,[27,28] where the structural parameters for **P4-X** were obtained from the MD minimization. The overall CD was estimated as a sum of exciton interactions between each pair of pyrenes, yielding the simulated CD shown in Fig. 6. This spectrum closely resembled the shape of the experimentally observed CD. Therefore, the CD simulations strongly suggest that the covalently attached pyrenes can associate helically along the minor groove of the RNA duplex.

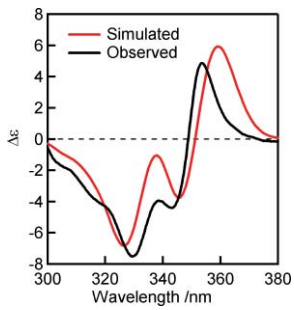

Fig. 6 Simulated CD spectrum of **P4-X** obtained from the exciton-chirality method using four Gaussians to simulate the absorption band of the pyrenyl group.

Since the CD observation and the CD simulation revealed that the exciton-coupled CD signal of the multiple-pyrene-modified RNA duplexes depended on the number of associations and the manner of association, the following is suggested for the pyrene association in **Qn-Y** ($n = 2$–4) and **Rn-Z**s ($n = 2$–3) systems. The shape of the exciton-coupled CD for **Qn-Y** ($n = 2$–4) was similar to that for **Pn-X** ($n = 2$–4), indicating that the manner of association of pyrenes in **Qn-Y** was similar to that in **Pn-X**. Hence, the manner of association of pyrenes in consecutive $\mathbf{U}_{py}$ domains was independent of the position of the domains and the context sequence of the consecutive $\mathbf{U}_{py}$ domains. In the **Rn-Z** system, the pyrene-modified duplex **R2-Z** containing $\mathbf{U}_{py}$ and $\mathbf{C}_{py}$ also showed similar exciton-coupled CDs to those of **P2-X** and **Q2-X**. This indicates that the manner of association of pyrenes in the $\mathbf{C}_{py}\mathbf{U}_{py}$ domain was similar to that in the $\mathbf{U}_{py}\mathbf{U}_{py}$ domain because $\mathbf{U}_{py}$ and $\mathbf{C}_{py}$ have a pyrimidine nucleobase. On the other hand, the shape of the exciton-coupled CD signal of **R3-Z** containing $\mathbf{U}_{py}$, $\mathbf{C}_{py}$, and $\mathbf{A}_{py}$ differed from those of other multiple-pyrene-modified RNA duplexes. Because the manner of association of pyrene in purine nucleotides such as $\mathbf{A}_{py}$ is probably different from that in pyrimidine nucleotides, such as $\mathbf{U}_{py}$ and $\mathbf{C}_{py}$, the addition of $\mathbf{A}_{py}$ to the $\mathbf{C}_{py}\mathbf{U}_{py}$ domain will probably induce changes in exciton-coupled CD signals. Further research is necessary to confirm this.

Conclusions

We demonstrated that multiple-pyrene-modified RNA duplexes had pyrene structures in helical association along the minor groove of the RNA duplexes. The pyrene association showed that the exciton-coupled CD signals and pyrene excimer fluorescence had intensities depending on RNA sequences and contexts. These findings will improve insight into sequence design of

pyrene-modified RNAs for the development of new materials and biotechnological applications.

Experimental

General methods

^{1}H NMR spectra were recorded on a Bruker DRX-500 spectrometer, in which chemical shifts (δ ppm) were determined on the basis of a residual peak of solvent (2.49 for DMSO-d_6). Absorption spectra in solution were recorded on a Hitachi U-3500 spectrophotometer, steady-state fluorescence spectra in solution were measured on a Hitachi F-2500 spectrofluorometer using excitation and emission slits of 5 nm and corrected. Thermal denaturations of RNA duplexes were carried out using a Bechman Coulter Du800. CD spectra were recorded on a JASCO 715 spectropolarimeter.

Syntheses of pyrene modified phosphoramidite monomer according to Scheme 1

2′-*O*-(Pyren-1-ylmethyl)-adenosine (1). 1-Pyrenyl methyl chloride (1.3 g, 5.16 mmol) was added to a solution of adenosine (2.1 g, 7.74 mmol) and NaH (0.28 g) in DMF (40 ml). The reaction mixture was stirred overnight at room temperature and then 10 ml of water were added to the solution. Dichloromethane (150 ml) was then added to the solution and the solution was washed with water. The organic layer was dried over Na_2SO_4 and then evaporated to near dryness. The residual material was purified by silica gel column chromatography with dichloromethane containing methanol (9 : 1, CH_2Cl_2–MeOH, v/v). Yield, 23% (0.57 g); TLC (9 : 1, CH_2Cl_2–MeOH, v/v), R_f 0.29; ^{1}H-NMR (DMSO-d_6): 3.59 (m, 1H, 5′-CH_2), 3.78 (m, 1H, 5′-CH_2), 4.07 (m, 1H, 4′-CH), 4.50 (m, 1H, 3′-CH), 4.79 (dd, 1H, 2′-CH), 5.16 (d, 1H, CH_2-pyrene), 5.43 (d, 1H, CH_2-pyrene), 5.52 (d, 1H, 3′-OH), 6.11 (d, 1H, 1′-CH), 7.30 (s, 2H, NH_2), 7.95–8.24 (m, total 9H, pyrene), 8.32 (s, 1H, adenine) and 8.51 (s, 1H, adenine).

2′-*O*-(Pyren-1-ylmethyl)-*N*-benzoyl-adenosine (2). Trimethylsilyl chloride (0.66 ml, 5.19 mmol) was added to a solution of **1** (0.5 g, 1.04 mmol), which was dried by coevaporation with pyridine three times, in pyridine (10 ml). After stirring for 30 min, benzoyl chloride (0.36 ml, 3.1 mmol) was added to the solution. The solution was stirred for 7 h at room temperature, and 10 ml of 28% NH_3 aqueous solution was added to the solution. After stirring for 1 h, the solution was concentrated to near dryness. The residual material was dissolved in dichloromethane (150 ml) and was then washed with water. The organic phase was dried over Na_2SO_4 and then evaporated to near dryness. The product **2** was purified by silica gel column chromatography with dichloromethane containing methanol (9 : 1, CH_2Cl_2–MeOH, v/v). Yield, 93% (0.90 g); TLC (9 : 1, CH_2Cl_2–MeOH, v/v), R_f 0.56; ^{1}H-NMR (DMSO-d_6): 3.61 (m, 1H, 5′-CH_2), 3.69 (m, 1H, 5′-CH_2), 4.09 (m, 1H, 4′-CH), 4.53 (m, 1H, 3′-CH), 4.83 (dd, 1H, 2′-CH), 5.19–5.21 (m, total 2H, 5′-OH and CH_2-pyrene), 5.50 (d, 1H, CH_2-pyrene), 5.60 (d, 1H, 3′-OH), 6.23 (d, 1H, 1′-CH), 7.56 (dd, 2H, aromatic of benzoyl), 7.62 (dd, 1H, aromatic of benzoyl), 7.96–8.26 (m, total 11H, aromatic of benzoyl and pyrene), 8.54 (s, 1H, adenine), 8.59 (s, 1H, adenine) and 11.09 (s, 1H, amide).

5′-Dimethoxytrityl-2′-*O*-(pyren-1-ylmethyl)-*N*-benzoyl-adenosine (3). 4,4′-Dimethoxytrityl chloride (0.43 g, 1.28 mmol) was added to a solution of **2** (0.43 g, 0.73 mmol), which was dried by coevaporation with pyridine three times, in pyridine (4.3 ml). After stirring for 6 h at room temperature, the solution was concentrated to near dryness. The residual material was dissolved in dichloromethane (150 ml) and then washed with water. The organic phase was dried over Na_2SO_4 and evaporated to near dryness. The product **3** was purified with silica gel column chromatography with dichloromethane containing methanol (9 : 1, CH_2Cl_2–MeOH, v/v). The appropriate fractions were pooled and then evaporated to near dryness. The residual solution was poured into cooled hexane and the precipitate was collected. Yield, 56% (0.29 g); TLC (9 : 1, CH_2Cl_2–MeOH, v/v), R_f 0.78; ^{1}H-NMR (DMSO-d_6): 3.68 (s, 6H, OCH_3), 4.19 (m, 1H, 4′-CH), 4.60 (m, 1H, 3′-CH), 4.96 (dd, 1H, 2′-CH), 5.26 (d, 1H, CH_2-pyrene), 5.49 (d, 1H, CH_2-pyrene), 5.60 (d, 1H, 3′-OH), 6.25 (d, 1H, 1′-CH), 6.79 (d, 4H, aromatic of DMT), 7.15–7.23 (m, total 7H, aromatic of DMT), 7.33 (d, 2H, aromatic of DMT), 7.56 (dd, 2H, aromatic of benzoyl), 7.62 (dd, 1H, aromatic of benzoyl), 7.99–8.26 (m, total 11H, aromatic of benzoyl and pyrene), 8.43 (s, 1H, adenine), 8.47 (s, 1H, adenine) and 11.08 (s, 1H, amide).

5′-Dimethoxytrityl-2′-*O*-(pyren-1-ylmethyl)-*N*-benzoyl-adenosine, 3′-{(2-cyanoethyl)-(*N*,*N*-diisopropyl)}-phosphoramidite (4). 2-Cyanoethyl-*N*,*N*,*N*′,*N*′-tetraisopropylphosphateamidite (0.07 ml, 0.2 mmol) was added to a solution of **3** (0.13 g, 0.15 mmol) and tetrazole (0.01 g, 0.15 mmol) in dry dichloromethane (1 mL). The solution was stirred for 2 h at room temperature and then dichloromethane (5 ml) was added to the solution. The solution was washed with 10% $NaHCO_3$ aqueous solution, dried over Na_2SO_4 and then evaporated to near dryness. The product **4** was purified by silica gel column chromatography with dichloromethane containing ethyl acetate and triethylamine (45 : 45 : 10, CH_2Cl_2–AcOEt–Et_3N, v/v). Yield, 89% (0.31 g); TLC (45 : 45 : 10, CH_2Cl_2–AcOEt–Et_3N, v/v), R_f 0.75.

2′-*O*-(Pyren-1-ylmethyl)-cytidine (5). 1-Pyrenyl methyl chloride (2.0 g, 8.0 mmol) was added to a solution of cytidine (2.9 g, 12.0 mmol) and NaH (0.43 g) in DMF (60 ml) at 0 °C. The reaction mixture was stirred overnight at room temperature and then 10 ml of water were added to the solution. Dichloromethane (150 ml) was then added to the solution and the solution was washed with water. The organic layer was dried over Na_2SO_4 and then evaporated to near dryness. The residual material was purified by silica gel column chromatography with dichloromethane containing methanol (9 : 1, CH_2Cl_2–MeOH, v/v). Yield, 44% (1.62 g); TLC (9 : 1, CH_2Cl_2–MeOH, v/v), R_f 0.33; ^{1}H-NMR (DMSO-d_6): 3.60 (m, 1H, 5′-CH_2), 3.69 (m, 1H, 5′-CH_2), 3.93 (m, 1H, 4′-CH), 4.07 (dd, 1H, 2′-CH), 4.19 (m, 1H, 3′-CH), 5.11 (m, 1H, 5′-OH), 5.22 (d, 1H, 3′-OH), 5.24 (d, 1H, CH_2-pyrene), 5.39 (d, 1H, CH_2-pyrene), 5.67 (d, 1H, cytosine), 6.06 (d, 1H, 1′-CH), 7.16 (s, 2H, NH_2), 7.90 (d, 1H, cytosine) and 8.08–8.31 (m, total 9H, aromatic of pyrene).

2′-*O*-(Pyren-1-ylmethyl)-*N*-benzoyl-cytidine (6). Trimethylsilyl chloride (0.69 ml, 5.45 mmol) was added to a solution of **5** (0.5 g, 1.1 mmol), which was dried by coevaporation with pyridine three times, in pyridine (10 ml). After stirring for 30 min, benzoyl chloride (0.38 ml, 3.3 mmol) was added to the solution. The solution was stirred for 7 h at room temperature, and then 10 ml of

28% NH_3 aqueous solution was added to the solution at 0 °C. After stirring for 1 h, the solution was concentrated to near dryness. The residual material was dissolved in dichloromethane and then washed with water. The organic phase was dried over Na_2SO_4 and evaporated to near dryness. Silica gel column chromatography of the residual material gave pure **6** with dichloromethane containing methanol (9 : 1, CH_2Cl_2–MeOH, v/v) as eluent. Yield, 47% (0.29 g); TLC (9 : 1, CH_2Cl_2–MeOH, v/v), R_f 0.49; ^{1}H-NMR (DMSO-d_6): 3.63 (m, 1H, 5′-CH_2), 3.75 (m, 1H, 5′-CH_2), 4.01 (m, 1H, 4′-CH), 4.16 (dd, 1H, 2′-CH), 4.24 (m, 1H, 3′-CH), 5.21 (m, 1H, 5′-OH), 5.32 (d, 1H, 3′-OH), 5.43 (d, 1H, CH_2-pyrene), 5.52 (d, 1H, CH_2-pyrene), 6.12 (d, 1H, 1′-CH), 7.44 (d, 1H, cytosine), 7.52 (dd, 2H, aromatic of benzoyl), 7.62 (dd, 1H, aromatic of benzoyl), 7.85 (d, 1H, cytosine), 8.00–8.30 (m, total 11H, aromatic of benzoyl and pyrene) and 11.18 (s, 1H, amide).

5′-Dimethoxytrityl-2′-*O*-(pyren-1-ylmethyl)-*N*-benzoyl-cytidine (7). 4,4′-Dimethoxytrityl chloride (0.36 g, 0.82 mmol) was added to a solution of **6** (0.46 g, 0.82 mmol), which was dried by coevaporation with pyridine three times, in pyridine (4.1 ml). The solution was stirred for 6 h at room temperature and then concentrated to near dryness. The residual material was dissolved in dichloromethane and then washed with water. The organic phase was dried over Na_2SO_4 and evaporated to near dryness. The product **7** was purified with silica gel column chromatography with dichloromethane containing methanol (9 : 1, CH_2Cl_2–MeOH, v/v). The appropriate fractions were pooled and then evaporated to near dryness. The residual solution was poured into cooled hexane and then the precipitate was collected. Yield, 50% (0.35 g); TLC (9 : 1, CH_2Cl_2–MeOH, v/v), R_f 0.88; ^{1}H-NMR (DMSO-d_6): 3.70 (s, 6H, OCH_3), 4.11–4.18 (m, total 2H, 2′-CH and 4′-CH), 4.43 (m, 1H, 3′-CH), 5.44 (m, 1H, 3′-OH), 5.55 (s, 2H, CH_2-pyrene), 6.13 (d, 1H, 1′-CH), 6.86 (d, 4H, aromatic of DMT), 7.21–7.30 (m, total 9H, aromatic of DMT), 7.36 (d, 1H, cytosine), 7.53 (dd, 2H, aromatic of benzoyl), 7.63 (dd, 1H, aromatic of benzoyl), 7.97 (d, 1H, cytosine), 8.02–8.32 (m, total 11H, aromatic of benzoyl and pyrene) and 11.21 (s, 1H, amide).

5′-Dimethoxytrityl-2′-*O*-(pyren-1-ylmethyl)-*N*-benzoyl-cytidine, 3′-{(2-cyanoethyl)-(*N*,*N*-diisopropyl)}-phosphoramidite (8). 2-Cyanoethyl-*N*,*N*,*N*′,*N*′-tetraisopropylphosphateamidite (0.17 ml, 0.53 mmol) was added to a solution of **7** (0.35 g, 0.41 mmol) and tetrazole (0.03 g, 0.41 mmol) in dry dichloromethane (1 mL). The solution was stirred for 2 h at room temperature and then dichloromethane (5 ml) was added to the solution. The solution was washed with 10% $NaHCO_3$ aqueous solution, dried over Na_2SO_4 and then evaporated to near dryness. The product **8** was purified by silica gel column chromatography with dichloromethane containing ethyl acetate and triethylamine (45 : 45 : 10, CH_2Cl_2–AcOEt–Et_3N, v/v). Yield, 88% (0.39 g); TLC (45 : 45 : 10, CH_2Cl_2–AcOEt–Et_3N, v/v), R_f 0.67.

RNA syntheses

All the RNAs were prepared by conventional phosphoramidite chemistry using an automated DNA synthesizer. After the recommended workup, they were purified by reversed-phase HPLC and characterized by UV–vis absorption and fluorescence spectroscopy.

MD simulation

The modified nucleoside, 2′-*O*-(1-pyrenylmethyl)uridine, was constructed using a support program for AMBER on the basis of our originally developed molecular graphics program. Formal charges for the modified nucleoside were calculated by MOPAC, and each atom in the pyrenyl residue was defined for molecular model building using "parm94" for AMBER.[26] The starting model for **P4-X** was optimized, thermalized (300 K) and equilibrated before MD simulation. The equilibrated structures were neutralized by adding a suitable number of Na^+ ions and solvated in rectangular boxes containing about 5400 of TIP3P water molecules such that the minimum distance from the duplex to the periodic boundary was 10 Å. The MD simulation of **P4-X** was performed using the "sander" module of the AMBER 7.0 software package with an appropriate force field.

Theoretical CD calculation

In this work, the absorption bands of pyrene were deconvoluted into four vibronic peaks. Each vibronic peak was regarded as a separate transition and fitted with a Gaussian function.[29] The transition dipole moment for the ^1L_a band was assumed to be polarized in the direction of the long axis as an ^1L_a band and to be common among all the vibronic peaks in the ^1L_a band. The magnitude of the transition dipole moment for each vibronic peak was determined from UV absorption. Each transition dipole moment vector was placed in the center of the pyrene ring. The mutual orientation of the transition dipole moments of the neighboring pyrene groups and their positions were determined from the geometries obtained by the MD minimized structure. Only the interactions between the like transitions were taken into consideration and the overall CD was estimated as a sum of exciton interactions between various pairs of pyrenes.

Acknowledgements

The authors thank Prof. Yoshihisa Inoue and Dr Hideo Nishino for measurements of CD spectra. This research was supported by a Grant-in-Aid for Scientific Research from JSPS.

Notes and references

1 J. Gao, C. Strassler, D. Tahmassebi and E. T. Kool, *J. Am. Chem. Soc.*, 2002, **124**, 11590.
2 H. Asanuma, K. Shirasuka, T. Takarada, H. Kashida and M. Komiyama, *J. Am. Chem. Soc.*, 2003, **125**, 2217.
3 K. Tanaka, A. Tengeiji, T. Kato, N. Toyama and M. Shionoya, *Science*, 2003, **299**, 1212.
4 K. Tanaka and M. Shionoya, *Chem. Lett.*, 2006, **35**, 694.
5 I. Dilek, M. Madrid, R. Singh, C. P. Urrea and B. A. Armitage, *J. Am. Chem. Soc.*, 2005, **127**, 3339.
6 H. Baruah, C. S. Day, M. W. Wright and U. Bierbach, *J. Am. Chem. Soc.*, 2004, **126**, 4492.
7 L. M. Scolaro, A. Romeo and R. F. Pasternack, *J. Am. Chem. Soc.*, 2004, **126**, 7178.
8 A. Furstenberg, M. D. Julliard, T. G. Deligeorgiev, N. I. Gadjev, A. A. Vasilev and E. Vauthey, *J. Am. Chem. Soc.*, 2006, **128**, 7661.
9 M. Wang, G. L. Silva and B. A. Armitage, *J. Am. Chem. Soc.*, 2000, **122**, 9977.
10 R. A. Caldwell, D. Creed, D. C. DeMarco, L. A. Melton, H. Ohta and P. H. Wine, *J. Am. Chem. Soc.*, 1980, **102**, 2369.
11 N. E. Geacintov, T. Prusik and M. J. Khosrofian, *J. Am. Chem. Soc.*, 1976, **98**, 6444.

12 V. Y. Shafirovich, S. H. Courtney, N. Ya and N. E. Geacintov, *J. Am. Chem. Soc.*, 1995, **117**, 4920.
13 Y. Cho and E. T. Kool, *ChemBioChem*, 2006, **7**, 669.
14 E. M. Enhart and H.-A. Wagenknecht, *Angew. Chem., Int. Ed.*, 2006, **45**, 3372.
15 J. Barbaric and H.-A. Wagenknecht, *Org. Biomol. Chem.*, 2006, **4**, 2088.
16 P. J. Hrdlicka, B. R. Babu, M. D. Sorensen, N. Harrit and J. Wengel, *J. Am. Chem. Soc.*, 2005, **127**, 13293.
17 M. Kosuge, M. Kubota and A. Ono, *Tetrahedron Lett.*, 2004, **45**, 3945.
18 A. Mahara, R. Iwase, T. Sakamoto, K. Yamana, T. Yamaoka and A. Murakami, *Angew. Chem., Int. Ed.*, 2002, **41**, 3648.
19 K. Yamana, H. Zako, K. Asazuma, R. Iwase, H. Nakano and A. Murakami, *Angew. Chem., Int. Ed.*, 2001, **40**, 1104.
20 M. Nakamura, Y. Ohtoshi and K. Yamana, *Chem. Commun.*, 2005.
21 K. Yamana, R. Iwase, S. Furutani, H. Tsuchida, H. Zako, T. Yamaoka and A. Murakami, *Nucleic Acids Res.*, 1999, **27**, 2387.
22 F. D. Saeva, P. E. Sharpe and G. R. Olin, *J. Am. Chem. Soc.*, 1973, **95**, 7656.
23 R. M. Hochstrasser, *J. Chem. Phys.*, 1960, **33**, 459.
24 W. C. Johnson, in *Circular Dichroism*, ed. N. Berova, K. Nakanishi and R. W. Woody, VCH, New York, 2nd edn, 2000, ch. 24, pp. 703–718.
25 M. Nakamura, Y. Fukunaga, K. Sasa, Y. Ohtoshi, K. Kanaori, H. Hayashi, H. Nakano and K. Yamana, *Nucleic Acids Res.*, 2005, **33**, 5887.
26 W. D. Cornell, P. Cieplak, C. I. Bayly, I. R. Gould, K. M. Merz, M. D. Ferguson, D. C. Spellmeyer, T. Fox, J. W. Caldwell and P. A. Kollman, *J. Am. Chem. Soc.*, 1995, **117**, 5179.
27 N. Harada, K. Nakanishi, *Circular Dichroic Spectroscopy: Exciton Coupling in Organic Stereochemistry*, University Science Books, New York, 1982.
28 N. Berova, K. Nakanishi, in *Circular Dichroism*, ed. N. Berova, K. Nakanishi and R. W. Woody, VCH, New York, 2nd edn, 2000, ch. 12, pp. 337–382.
29 F. D. Lewis, L. Zhang, X. Liu, X. Zuo, D. M. Tiede, H. Long and G. C. Schatz, *J. Am. Chem. Soc.*, 2005, **127**, 14445.